MULTISPECTRAL TEXTURE ANALYSIS USING LOCAL BINARY PATTERN ON TOTALLY ORDERED VECTORIAL SPACES

Vincent Barra
LIMOS, UMR 6158, Campus des Cézeaux, 63173 Aubière, France

Keywords: Local binary pattern, Multispectral image, Segmentation, Texture, Total orderings.

Abstract: Texture is an important feature when considering image segmentation. Since more and more image segmentation problems involve multi- and hyperspectral data, including color images, it becomes necessary to define multispectral texture features. In this article, we propose LMBP, an extension of the classical Local Binary Pattern (LBP) operator to the case of multispectral images. The LMBP operator is based on the definition of total orderings in the image space and on an extension of the standard univariate LBP. It allows the computation of both a multispectral texture structure coefficient and a multispectral contrast parameter for each spatial location, that serve as an input to an unsupervised clustering algorithm. Results are demonstrated in the case of the segmentation of brain tissues from multispectral MR images, and compared to other multispectral texture features.

1 INTRODUCTION

Texture analysis plays an important role in several applications, from remote sensing to medical image processing, industrial applications or document processing. Four major issues are expected in texture analysis: feature extraction, texture discrimination, texture classification and shape from texture. To achieve these analysis, several methods are available, using statistical (autocorrelation, co-occurrence), geometrical (structural techniques), model-based (MRF or fractal) or signal processing based approaches (spatial,Fourier, Gabor or wavelet filtering) (see for example (Tuceryan and Jain, 1998) for a review). Among all these methods, the Local Binary Pattern (LBP) operator offers an efficient way of analyzing textures (Ojala et al., 2002). It relies on a simple but efficient theoretical framework, and combines both structural and statistical properties.

In the prementioned potential applications, color and even multispectral data is more and more available and the extension of texture analysis methods becomes natural. We propose in this article to extend the LBP operator to the case of multispectral images. Contrary to other works (Lucieer et al., 2005; Song et al., 2006), we do not apply the univariate LBP on scalar values derived from the multispectral dataset, but directly propose a multispectral LBP operator, based on a total ordering computed either in the images space, or in a derived vectorial space.

The paper is organized as follows: Section 2 first recall the original univariate LBP operator, and recall some basic definitions on orderings in a vectorial space. It then introduces the LMBP - Local Multispectral Binary Pattern, that uses both of these notions. Section 3 presents and analyzes some preliminary results of the operator on data stemming from multispectral Magnetic Resonance Images.

2 LOCAL MULTISPECTRAL BINARY PATTERN

2.1 Local Binary Pattern

Ojala et al. (Ojala et al., 2002) described the texture T as the joint distribution of the gray levels of $P+1$ image pixels: $T = t(g_c, g_0 \cdots g_{p-1})$, where g_c is the gray level value of the center pixel, surrounded by P equally spaces pixels of gray levels g_p, located on a circle of radius R. Gray values g_p were interpolated if neighbors didn't fit on the pixel grid. They then defined the Local Binary Pattern (LBP), a grayscale invariant and rotation invariant operator:

$$LBP_{P,R}^{riu2} = \begin{cases} \sum_{i=0}^{P-1} \sigma(g_p - g_c) & \text{if } U(LBP_{P,R}) \leq 2 \\ P+1 & \text{otherwise} \end{cases}$$

where

Barra V. (2010).
MULTISPECTRAL TEXTURE ANALYSIS USING LOCAL BINARY PATTERN ON TOTALLY ORDERED VECTORIAL SPACES.
In *Proceedings of the International Conference on Computer Vision Theory and Applications*, pages 37-43
DOI: 10.5220/0002828700370043

$$U(LBP_{P,R}) = |\sigma(g_{P-1}-g_c) - \sigma(g_0 - g_c)| + \sum_{i=1}^{P-1} |\sigma(g_i - g_c) - \sigma(g_{i-1}-g_c)|$$

and $\sigma(.)$ is the sign function. The uniformity function $U(LBP_{P,R})$ corresponds to the number of spatial transitions in the neighborhood: the larger it is, the more likely a spatial transition occurs in the local pattern.
If $LBP_{P,R}^{riu2}$ captures the spatial structure of the texture, it does not handle the strength of the pattern. To do so, a contrast measure was defined as

$$C_{P,R} = \frac{1}{P}\sum_{i=0}^{P-1}(g_i - \bar{g})^2 \quad \text{where} \quad \bar{g} = \frac{1}{P}\sum_{i=0}^{P-1} g_i$$

and textures may then be characterized by the joint distribution of $LBP_{P,R}^{riu2}$ and $C_{P,R}$.
Several extensions have been proposed to these features (e.g. multi-resolution LBP (Mäenpää and Pietikäinen, 2003; Ojala et al., 2002), center-symmetric local binary pattern (Heikkilä et al., 2009)), and numerous applications have been adressed using these techniques (e.g. face recognition (Ahonen et al., 2006), segmentation of remote-sensing images (Wang and Wang, 2006), visual inspection (Paclik et al., 2002) or classification of outdoor images (García and Puig, 2007)).

The LBP operator relies on the sign function $\sigma(.)$, and then on an ordering relation on the gray level space. Since there is no natural ordering for vector spaces, such as those produced by multispectral imaging, the extension of LBP to multispectral data is not straightforward. Some authors already defined multispectral LBP by combining intra-plane and inter-plane LBP relations (Lucieer et al., 2005), or by considering the univariate LBP on vector norms (Song et al., 2006), but to our knowledge no LBP operator has directly be defined on vectorial data. We thus propose in the following to define the LMBP - Local Multispectral Binary Pattern - operator, based on LBP and on total orderings on $\mathbb{R}^n$. We first recall basic definitions on orders and then introduce the LMBP operator.

2.2 Total Orderings in $\mathbb{R}^n$

We first recall some basic definitions.

Definition 1. *Let $\leq_P$ be a binary relation on a set P. $\leq_P$ is a pre-order if it is:*

- *reflexive:* $(\forall x \in P) \quad x \leq_P x$
- *transitive: for all $x,y,z \in P$, if $x \leq_P y$ and $y \leq_P z$ then $x \leq_P z$*

Definition 2. *Let $\leq_P$ be a binary relation on a set P. $\leq_P$ is a partial order if it is a pre-order and for all $x,y \in P$, if $x \leq_P y$ and $y \leq_P x$ then $x = y$ (antisymmetry)*

Definition 3. *Let $\leq_P$ be a partial order on a set P. $\leq_P$ is a total order if and only if for all $x,y \in P$, $x \leq_P y$ or $y \leq_P x$*

If it is straightforward to define orders for scalar values, the definition of partial -or total- orders for vector valued data is not so easy: if data stems from RGB images ($P = \mathbb{R}^3$), each channel being coded on 8 bits, each pixel can have one of the 2^{24} possible vectorial values, hence defining $2^{24}!$ possible total orderings.
One has then to find another way to introduce order in $\mathbb{R}^n$. Barnett (Barnett, 1976) defined four ways to order vectors: the marginal approach, the partial approach, the conditional order and the dimension reduction. This last technique is an usual way to proceed, (Goutsias et al., 1995), and consists either in defining an order using a distance in $\mathbb{R}^n$ of each vector to a reference, or in projecting vectors into a vectorial space $\mathbb{R}^q$ where an order can be defined. In this latter case, the projection is defined by an application $h : \mathbb{R}^n \to \mathbb{R}^q$, and (Chanussot and Lambert, 1998) proved that :

- h defines an ordering relation $\leq_n$ in $\mathbb{R}^n$ if and only if h is injective (and h can be supposed to be bijective if $\mathbb{R}^q$ is restricted to $h(\mathbb{R}^n)$)
- $\leq_n$ defines a total order in $\mathbb{R}^n$ if and only if there exist $h : \mathbb{R}^n \to \mathbb{R}^q$ bijective defining $\leq_n$ on $\mathbb{R}^n$ and q=1
- $\leq_n$ defines a total order in $\mathbb{R}^n$ if and only if $\leq_n$ defines a space filling curve of $\mathbb{R}^n$

Total ordering may then be identically handled by the definition of h, or by the construction of a space filling curve of $\mathbb{R}^n$. In the following, we propose as a preliminary study to define $\leq_n$ using an appropriate h.

2.3 The LMBP Operator

Figure 1 presents an overview of the algorithm. Each step is detailed in the following subsections

2.3.1 Subspace Analysis

Since numerous information may be available from the original dataset of $\mathbb{R}^p$, and since the p original images may be dependent, it may be useful to conduct feature extraction before defining the vector ordering. Several techniques are available to extract

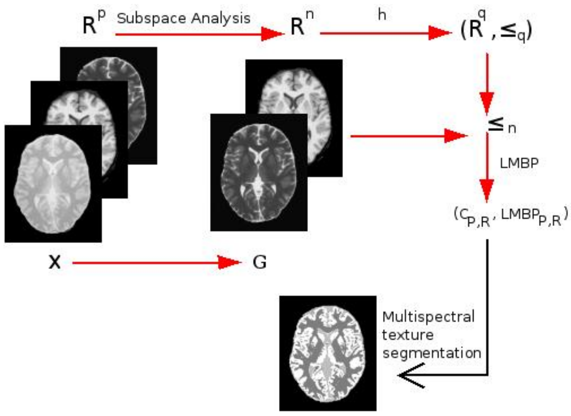

Figure 1: Overview of the algorithm.

features (Principal or Independent Component Analysis, Minimum Noise Fraction, or nonlinear techniques such as Isomap or Local Linear Embedding). In a preliminary study, we used a simple and linear technique, the Principal Component Analysis (PCA), that will directly impact the choice of the h function: if $X \in \mathcal{M}_{m,p}(\mathbb{R})$ denotes the matrix of the original data (m being the number of pixels, p the number of images and $X_{.,i}$ the i^{th} column of X), the principal components are computed from the projections of the original data onto the eigenvectors of Z^TZ, where $Z = (X - \mathbf{1}\mu)D$ is the matrix of centered and reduced data, $\mathbf{1} = (1 \cdots 1) \in \mathbb{R}^m, \mu = (\bar{X_{.,1}} \cdots \bar{X_{.,p}}) \in \mathbb{R}^p$ is the vector of image mean values and $D = diag(1/s_i)$, $s_i, 1 \leq i \leq p$ is the standard deviation of variable i. PCA allows $n < p$ new variables to be computed, explaining most of the variance of the original data. The resulting information is stored in $G \in \mathcal{M}_{m,n}(\mathbb{R})$.

2.3.2 Definition of h

Recall that $h : \mathbb{R}^n \rightarrow \mathbb{R}^q$, an easily way to compute an ordering relation in $\mathbb{R}^n$ is to derive it from h using the canonical ordering relation of $\mathbb{R}^q, q \geq 1$:

$$x \leq_q y \Leftrightarrow (\forall 1 \leq i \leq q, x(i) \leq y(i))$$

This ordering relation is a partial order, and in the context of image processing may lead to several drawbacks: some vectors may not be ordered, and notions of *Sup* and *Inf* are not defined (and are compulsory in areas such as mathematical morphology). In our context, we thus decide to define a total ordering in $\mathbb{R}^n$, then using $q = 1$ and h injective. Several choices are possible (*e.g.* the bit mixing approach (Chanussot and Lambert, 1998)), and we benefit from the new basis computed from PCA to use the lexicographic order in $\mathbb{R}^n$ defined as:

$$x \leq_n y \Leftrightarrow (\exists k \in \{1 \cdots n\})/x(i) = y(i), 1 \leq i \leq k-1, x(k) < y(k)$$

If each image is coded on b bits, the corresponding h function is

$$h(x) = \sum_{i=1}^{n} x(n+1-i)2^{b(i-1)}$$

2.3.3 Computation of LMBP

Once h has been defined, an ordering relation on $\mathbb{R}^n$ can be proposed as: $x \leq_n y \in \mathbb{R}^n \Leftrightarrow h(x) \leq h(y) \in \mathbb{R}$. Unfortunately, enforcing a total ordering on $\mathbb{R}^n$ makes h discontinuous: the Netto theorem (Sagan, 1994) indeed proved that any bijective application from a manifold of dimension n to a manifold of dimension $q \neq n$ is discontinuous. Thus, h is not a linear function, and does not commute with linear functions. It is thus not straightforward to assess $h(x) - h(y)$, given $x - y$ in $\mathbb{R}^n$, and any linear combination of vectors transformed by h should be avoided. If this is not really a problem for the definition of the LBP operator ($\sigma(g_p - g_c)$ should easily be replaced with $\sigma(h(g_p) - h(g_c))$ because the minus sign only means to compare $h(g_p)$ with $h(g_c)$ using the ordering defined by h), the extension of $C_{P,R}$ to the case of multispectral images is more problematic, because of both $\bar{g}$ and the deviation to this mean value. In order to be compliant with the discontinuity of h, we thus avoid any linear combination, and replace $\bar{g}$ by the median value m_p of the g_p's. The LBMP operator is then

$$LMBP_{P,R}^{riu2} = \begin{cases} \sum_{i=0}^{P-1} \sigma(h(g_p) - h(g_c)) & \text{if } U(LBP_{P,R}) \leq 2 \\ P+1 & \text{otherwise} \end{cases}$$

where

$$\begin{aligned} U(LBP_{P,R}) &= |\sigma(h(g_{P-1}) - h(g_c)) - \sigma(h(g_0) - h(g_c))| \\ &+ \sum_{i=1}^{P-1} |\sigma(h(g_i) - h(g_c)) - \sigma(h(g_{i-1}) - h(g_c))| \end{aligned}$$

and the contrast operator

$$C_{P,R} = \frac{1}{P} \sum_{i=0}^{P-1} (h(g_i) - h(m_p))^2$$

$C_{P,R}$ is still a combination of $h(g_i) - h(m_p)$, but we expect the nonlinearity introduced by m_p to reduce the discontinuity effects.
If h is computed from the lexicographic order, the sign functions $\sigma((h(x) - h(y)))$ in the previous expressions reduce to

$$\sigma(\sum_{j=1}^{n} (x(n+1-j) - y(n+1-j))\, 2^{b(j-1)})$$

The first components of x and y play here an important role, as their difference is weighted by $2^{b(n-1)}$, but the other components, with weights $2^{b.j}, j < n-1$ may invert the sign of the argument of the σ function. Subspace analysis is thus a crucial step in the whole process for the selection of relevant components.

2.3.4 From LMBP to Segmentation

Once LMBP and contrast have been computed for each pixel location, we were interested in image segmentation using these features. Several approaches can be performed, e.g.:

- incorporate these operators in a vector describing the pixel properties, with other relevant values (e.g. values of the first principal components). The set of these vectors then serves as an input of an unsupervised clustering algorithm
- compute a local 2D joint distribution (LMBP,$C_{P,R}$) for each pixel, and use an adapted metric to cluster pixels.

In this preliminary study, we chose to use the first alternative. More precisely, a classical K-means algorithm was used as a clustering method, using the Euclidean metric to cluster feature vectors that the next section will detail.

3 RESULTS

We apply the LMBP operator to the problem of multispectral MR image segmentation problem. As test data we used simulated MRI-datasets generated with the Internet connected *MRI Simulator* at the McConnell Brain Imaging Centre in Montreal (*www.bic.mni.mcgill.ca/brainweb/*). The datasets we used were based on an anatomical model of a normal brain that results from registering and preprocessing 27 scans from the same individual with subsequent semi-automated segmentation. In this dataset the different tissue types were well-defined, both "fuzzy" and "crisp" tissue membership were allocated to each voxel. From this tissue labeled brain volume the MR simulation algorithm, using discrete-event simulation of the pulse sequences based on the Bloch equations, predicted signal intensities and image contrast in a way that is equivalent to data acquired with a real MR-scanner. Both sequence parameters and the effect of partial volume averaging, noise, and intensity non-uniformity were incorporated in the simulation results (Cocosco et al., 1997; Kwan et al., 1999).
Ten multispectral (T1-weighted,T2-weighted, Proton density) MR datasets of a central slice (including the main brain tissues, basal ganglia and fine to coarse details), with variations of the parameters "noise" and "intensity non-uniformity (RF)" were chosen (table 1), the slice thickness being equal to 1mm. This selection covers the whole range of the parameter values available in *BrainWeb* so that the comparability with real data can be considered as sufficient to test the robustness of the method at varying image qualities.

Table 1: MR Datasets.

dataset no	dataset name	noise	RF
1	n1rf20	1%	20%
2	n1rf40	1%	40%
3	n3rf20	3%	20%
4	n3rf40	3%	40%
5	n5rf20	5%	20%
6	n5rf40	5%	40%
7	n7rf20	7%	20%
8	n7rf40	7%	40%
9	n9rf20	9%	20%
10	n9rf40	9%	40%

For obtaining the true volumes of brain tissues and background the corresponding pixels were counted in the ground truth image provided by *BrainWeb*.
We performed three types of analysis for each dataset, first transformed by a subspace analysis method (namely the PCA). More precisely, we characterized pixels with several types of feature vectors:

- either the vector of the first principal components, or a vector composed of the first principal components, the LMBP and the contrast operators (Interest of LMBP and Multispectral Contrast in the segmentation process, section 3.1).
- either a vector composed of the first principal components, the LMBP and the contrast operators, or a vector composed of the first principal components, the multispectral and the contrast operators as computed in (Song et al., 2006) (section 3.2)

In the following, we present results from dataset n9rf20 (figure 2) and use as LBP parameters $R = 1.5, P = 12$. All features were normalized by their max value to cluster homogeneous values.

3.1 Multispectral Texture Information

Figure 3 presents the results of the segmentation of the brain slice in 4 classes: background (BG, light gray), Cerebrospinal fluid (CSF, dark gray), white matter (WM, black) and gray matter (GM, white). S1 is the segmentation obtained with only the two first principal components, S2 with these two components plus the LMBP and the contrast operator values.

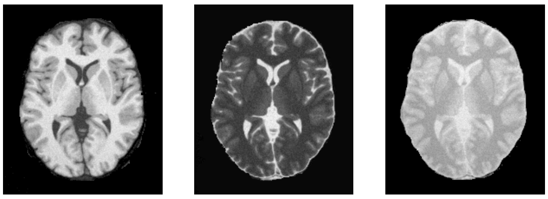

T1-weighted T2-weighted Proton Density

Figure 2: Slice of interest of dataset n9rf20.

In order to assess the two segmentations, we process the confusion matrix C on the segmented images: given a segmented image S, $C_S(i,j)$ is the percentage of pixels assigned to class $i \in \{BG, CSF, WM, GM\}$ in the ground truth and to class j in S. The closer C to a diagonal matrix, the better the segmentation is. Although segmented images seems to be the same, the confusion matrix reveal some differences:

$$C_{S1} = \begin{pmatrix} 48.4 & 10^{-1} & 1.8.10^{-3} & 0 \\ 0.44 & 4.64 & 1.58 & 0.83 \\ 0.06 & 0.12 & 19.28 & 4.62 \\ 0.13 & 0.89 & 0.71 & 18.2 \end{pmatrix}$$

$$C_{S2} = \begin{pmatrix} 48.3 & 0.10 & 2.10^{-2} & 0 \\ 0.46 & 5.73 & 0.56 & 0.88 \\ 0.05 & 0.05 & 19.28 & 4.63 \\ 0.13 & 0.87 & 0.45 & 18.45 \end{pmatrix}$$

The multispectral texture coefficients, and especially the LMBP operator, bring some information on structural properties on tissue edges: interfaces between tissues are more or less expressed depending on the acquisition (e.g. the CSF/(WM+GM) interface is very clear in T2-weighted images, whereas the proton density images better shows the WM/(GM+CSF) interface), and the multispectral structure of edges, seen as local oriented textures, is managed during the clustering process (figure 4). It is particularly visible for the WM/CSF interface between the corpus callosum and the lateral ventricles (see image and $C(2,3)$ coefficient) and for the WM/GM interface near the putamens (see image and $C(4,3)$ coefficient).

Table 2 shows the number of pixels assigned to each class. Relative errors for S1 (respectively S2) are 0.01 (0.01) for background, 0.31 (0.31) for CSF, 0.11 (0.06) for WM and 0.15 (0.11) for GM. For WM and GM, relative errors lower due to the integration of LBMP operators.

3.2 LMBP vs. Another Multispectral Texture Definition

We also compared the LMBP operator with a multispectral LBP already proposed in the litterature (Song et al., 2006), that compute LBP as:

Table 2: Number of pixels in each class.

	BG	CSF	WM	GM
truth	19826	2336	8741	9577
S1	19620	3039	9755	8066
S2	19601	3088	9328	8463

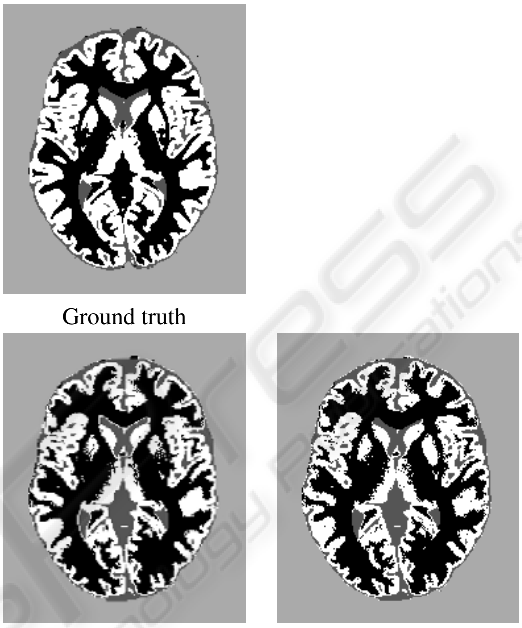

Ground truth

S1 S2

Figure 3: Segmentation results.

$$LBP_{P,R}^{riu2} = \begin{cases} \sum_{i=0}^{P-1} \sigma(\|g_p\| - \|g_c\|) & \text{if } U(LBP_{P,R}) \leq 2 \\ P+1 & \text{otherwise} \end{cases}$$

where norms also stand in the definition of U. As in (Song et al., 2006), we used the Euclidean norm, and the LBP parameters were chosen equal to those of LMBP. Note that this method is a particular case of LMBP, with $h : x \mapsto \|x\|$.

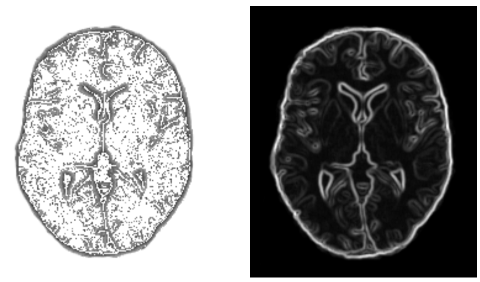

LBMP Contrast

Figure 4: LBMP and Contrast images.

Figure 5 shows LMBP and Contrast images for both methods, and figure 6 compares the two segmentations. Results were always much better using LMBP for all the MR volumes described in Table 1, and the difference increased as the noise increased in the image. The function $h : x \mapsto \|x\|$ used to produce the total ordering in $\mathbb{R}^n$ indeed tended to increase the lbp value in a noisy neighborhood of a pixel g_c, producing the noisy LBP image of figure 5.

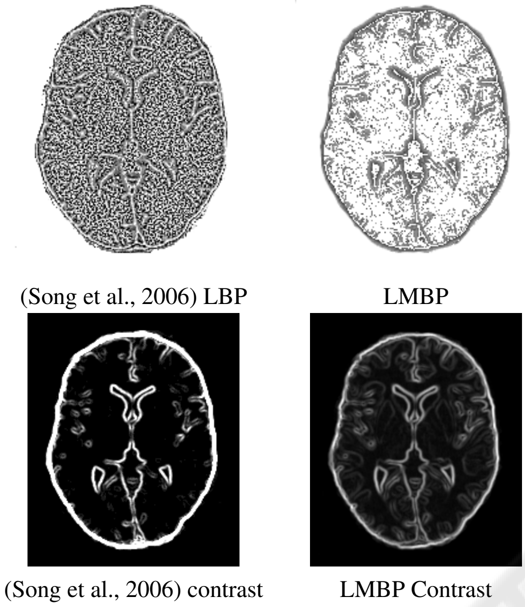

Figure 5: Comparison of multispectral LBP and Contrast images.

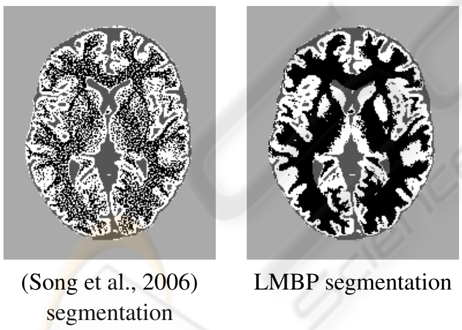

Figure 6: Comparison of segmentation results.

4 CONCLUSIONS

We proposed in this article a multispectral version of the classical Local Binary Pattern operator, based on a total ordering on the vectorial space of the data. We demonstrate its efficiency on multispectral MR images of the brain, assessing the results with respect to a ground truth, and comparing segmentation results with those provided by another multispectral LBP approach.

Numerous perspectives are now expected from this preliminary work. First of all, h needs to be better defined to allow the local topology to be preserved: two neighbors in $\mathbb{R}^n$ need to stay closed when transformed by h. For x and y neighbors in $\mathbb{R}^n$, the solution may be to define h using space filling curves directly on the multispectral image, in order to impose small variations of $h(x) - h(y)$ in areas of interest, and higher variations for example in the background.
The segmentation scheme also needs to be refine. For this study, standard techniques (PCA, Kmeans) were applied, and some work has now to be done to tune subspace analysis and segmentation methods to this specific problem. Finally, this multispectral approach finds natural applications not only in medical imaging, but also in remote sensing imagery. We now intend to tune and apply the LMBP to this domain.

REFERENCES

Ahonen, T., Hadid, A., and Pietikäinen, M. (2006). Face description with local binary patterns: Application to face recognition. *IEEE Trans. Pattern Anal. Mach. Intell.*, 28(12):2037–2041.

Barnett, V. (1976). The ordering of multivariate data. *Journal of the Royal Statistical Society, Series A*, 139:318–355.

Chanussot, J. and Lambert, P. (1998). Total ordering based on space filling curves for multivalued morphology. In *ISMM '98: Proceedings of the fourth international symposium on Mathematical morphology and its applications to image and signal processing*, pages 51–58, Norwell, MA, USA. Kluwer Academic Publishers.

Cocosco, C. A., Kollokian, V., Kwan, R. K. S., Pike, G. B., and Evans, A. C. (1997). Brainweb: Online interface to a 3d mri simulated brain database. *NeuroImage*, 5.

García, M. A. and Puig, D. (2007). Supervised texture classification by integration of multiple texture methods and evaluation windows. *Image Vision Comput.*, 25(7):1091–1106.

Goutsias, J. K., Heijmans, H. J. A. M., and Sivakumar, K. (1995). Morphological operators for image sequences. *Computer Vision and Image Understanding*, 62(3):326–346.

Heikkilä, M., Pietikäinen, M., and Schmid, C. (2009). Description of interest regions with local binary patterns. *Pattern Recogn.*, 42(3):425–436.

Kwan, R., Evans, A., and Pike, G. (1999). Mri simulation-based evaluation of image-processing and classification methods. 18(11):1085–1097.

Lucieer, A., Tsolmongerel, O., and Stein, A. (2005). Multivariate texture-based segmentation of remotely sensed images. *International Journal of Remote sensing*, 26:2917–2936.

Mäenpää, T. and Pietikäinen, M. (2003). Multi-scale binary patterns for texture analysis. pages 885–892.

Ojala, T., Pietikinen, M., and Menp, T. (2002). Multiresolution gray-scale and rotation invariant texture classification with local binary patterns. *IEEE Transactions on Pattern Analysis and Machine Intelligence*, 24(7):971–987.

Paclik, P., Duin, R. P., Kempen, G. M. P. V., and Kohlus, R. (2002). Supervised segmentation of textures in backscatter images. In *In: Proceedings of IEEE International Conference on Pattern Recognition*, pages 490–493. John Wiley and Sons.

Sagan, H. (1994). *Space Filling Curves*. Springer Verlag.

Song, C., Li, P., and Yang, F. (2006). Multivariate texture measured by local binary pattern for multispectral image classification. In *In: Proceedings of IEEE International Conference on Geoscience and Remote Sensing Symposium*, pages 2145–2148.

Tuceryan, M. and Jain, A. K. (1998). *Texture analysis*, volume 15 of *Handbook of Pattern Recognition and Computer Vision, Second Edition*, pages 207–248. World Scientific, c.h. chen, and l.f. pau edition.

Wang, A. P. and Wang, S. G. (2006). Content-based high-resolution remote sensing image retrieval with local binary patterns. In *Society of Photo-Optical Instrumentation Engineers (SPIE) Conference Series*, volume 6419 of *Society of Photo-Optical Instrumentation Engineers (SPIE) Conference Series*.